



## Corrosion and Wear Properties of Biodegradable Magnesium Alloy After Cold Rolling

Zaid Ali Hadi<sup>1</sup>, Zuheir Talib Khulief<sup>2\*</sup>

Department of Metallurgical Engineering, College of Materials Engineering, University of Babylon, Babylon 51002, Iraq

Corresponding Author Email: [mat.zuheir.talib@uobabylon.edu.iq](mailto:mat.zuheir.talib@uobabylon.edu.iq)

Copyright: ©2025 The authors. This article is published by IETA and is licensed under the CC BY 4.0 license (<http://creativecommons.org/licenses/by/4.0/>).

<https://doi.org/10.18280/mmep.120117>

### ABSTRACT

**Received:** 27 October 2023

**Revised:** 18 February 2024

**Accepted:** 25 February 2024

**Available online:** 25 January 2025

#### Keywords:

*cold rolling, corrosion, AZ91, biodegradable, magnesium alloy*

Biodegradable implants have become increasingly important in medical applications, and magnesium has emerged as a promising biomaterial due to the high specific strength, lightweight properties, cortical bone-like elasticity index, and high biocompatibility of magnesium alloy in this study (AZ91). The effect of different levels of cold working (rolling) on bio-corrosion wear properties is investigated. Samples were heated to 400°C for one hour and then cooled in an oven before being rolled separately weight loss (5%, 10%, 15%). Microstructure analysis was carried out using optical microscope and SEM to evaluate the effect of cold work on the treated samples. Wear tests were carried out by slitting the samples in simulated body fluid (SBF), while the samples were immersed in SBF and bio-corrosion was tested by measuring the corrosion rate using Tafel test and hydrogen evaluation. These findings have important implications in the development of biodegradable magnesium implants that improve performance and are biologically compatible.

## 1. INTRODUCTION

Magnesium alloys have great machinability and forging ability, making it possible to produce even the most difficult die-cast components with relative ease. Cast or solid magnesium alloy parts may be machined and welded using inert fuel. Magnesium alloys are highly sought-after materials because to their exceptional unique qualities, such as their low density (1.74 g/cm<sup>3</sup>) [1]. A major problem of magnesium alloys is the low corrosion resistance. Instead of forming a passive film to protect against corrosion as aluminum does, it has broken down completely. Magnesium and magnesium alloys have had their corrosion resistance improved upon in several ways since it is view as one of the material's fundamental flaws. Yet, the magnesium alloy's strong reactivity in corrosive conditions may find use in the biological realm [2]. Implants placed in hard tissues (temporary implant) nowadays always made of permanent materials such titanium alloys, Nitinol (55Ni-45Ti) or stainless steel. There may be consequences such as endothelial dysfunction, prolonged local inflammation, and pain. A second operation need to implant removed. As the human body is capable of mending and replacing injured tissue over time, a degradable implant Figure 1 would be the best course of therapy since it would give a physiologically less invasive temporary support and repair while the injured tissue healed. When its function has accomplished, this implant will naturally remove and expelled by the body [3]. The analysis controlled the amount of cold work during the freezing of the samples, mainly by decreasing the thicknesses by 5%, 10% and 15%. This allowed to investigate how cold work percentage this specificity is related to the materials studied.

The samples were initially heated to 400°C for one hour and then cooled in an oven prior to molding. Microstructure analysis was then performed using optical microscope and SEM to evaluate the effect of cold work on the samples. The controlled changes in thickness reduction have provided valuable insights into the relationship between cold working rates and consequent changes in wear resistance, microstructure and hardness.

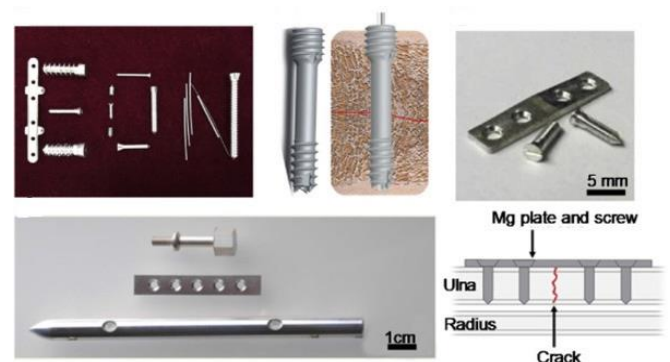


**Figure 1.** Medical device from magnesium and Mg alloys

## 2. LITERATURE REVIEW

This section previews the recent studies about bio-Mg alloys and shows the literature review summery. In 2015, Johnston et al. [4] studied hydrogen evolution and mass loss were used to analyze the corrosion of Magnesium high purity (HP), ZE41, and AZ91 in a CO<sub>2</sub>-bicarbonate buffered Hanks'

solution. The rate of corrosion is found to be as follows: ZE41 HP Mg AZ91. Compared to the other Mg alloys, ZE41 corroded at a substantially faster pace. Corrosion rate for AZ91 and HP Mg are similar, although HP Mg deteriorated more rapidly. As pH rose, protective coatings are more robust, and corrosion rates across the board reduced significantly. The corrosion rates of all Magnesium alloys are somewhat increased, and the corrosion morphology is uniformized, due to the sluggish fluid flow. In 2016, in the study conducted by Alsagabi et al. [5], specimens of AZ31 magnesium alloy are tested for electrochemical corrosion in room-temperature solutions of pH 4.5, 9.5, and 13.0 with additions of 0-2000 ppm of chloride. In solutions with a pH of 13 and up to 1500 ppm of chloride, cyclic polarization did not cause a loss of passivity. AZ31 corrosion in solutions with pH 4.5 and 9.5 is mitigated by adding supportive electrolytes sodium sulfate and sodium dihydrogen phosphate. The Mott-Schottky analysis revealed a duplex surface layer, with an n-type  $MgO_{1-x}$  inner layer ( $x=0.024-0.05$ ) and a p-type outer layer that grew with time at the cost of the inner layer. In 2017, Abbasi et al. [6] studied an electrolyte with varying sodium chloride and pH levels; see how pure magnesium and the magnesium alloy react to corrosion. This has been accomplished by using immersion and potentiodynamic polarization experiments with varying amounts of NaCl salt (3.5, 0.3, and 0.03 wt%). To learn how acidity and chloride ion concentration interact with one another to influence corrosion behavior, the pH of the electrolytes is held constant at 3, 6, and 11. It was discovered that the corrosion rate of the magnesium-like AZ31 alloy is higher and the open-circuit potential is more negative at higher chloride ion concentrations in each pH, and that the same trend is also observed at lower pH for each chloride ion concentration. The corrosion rate of an alloy in a given solution is inversely proportional to the pH of the solution, hence an increase in pH reduces corrosion. Chloride ion concentration changes have a larger effect than pH shifts in solutions. A thin protective layer controls the corrosion behavior of the magnesium alloy. Immersion test corrosion rates are predicted to be greater than polarization test rates for a number of reasons. In 2019, Liu et al. [7] demonstrated in their study that in order to achieve a nanostructured surface layer, AZ31 and AZ91 Mg alloys were subjected to severe shot peening (SP). Transmission electron microscopy, a micro-hardness tester, and corrosion tests are used to examine the microstructure, micro-hardness, and corrosion behavior of SP-treated AZ31 and AZ91 Mg alloys. A nanoscale plastic deformation layer including -Mg grains is found on the surface of AZ31 and AZ91 Mg alloys after SP treatment. Grain refinement and work hardening, both effects of SP treatment, clearly increased the micro-hardness in the near surface area for two alloys. By quickly forming a reasonably compact passive coating on the nanostructured surface, SP treatment increased AZ31 alloy's resistance to corrosion. Since SP treatment had only a modest impact on the size and distribution of -phases in AZ91 alloy, it is unable to significantly improve the material's corrosion resistance.

In 2020, Vaira Vignesh et al. [8] researched the effects of SBF on magnesium alloy corrosion and wear. Characterization of the microstructure and micro hardness of AZ91 magnesium alloy. Multiple types of corrosion tests, wear tests, and a combined corrosion-wear test were performed on the foundational material. The research found the following results: AZ91 is a magnesium alloy with a microstructure made up of eutectic phases of  $\alpha$ -Mg,  $\beta$ -Mg17Al12 and ( $\alpha+\beta$ ).

The  $\beta$  phase dispersed throughout the matrix as large, continuous precipitates. Time spent submerged in bodily fluids increases the likelihood that hydroxyapatite will develop on the AZ91D's surface. From the Tafel, we may extrapolate a corrosion potential of 1.448 V and a corrosion rate of 4.44 mm/year. Adhesive wear test statistical modeling sheds light on the relationship between the transition load and the evolution of wear-test variables. The wear test of samples is significantly affected by SBF. In 2023, Li et al. [9] researched a novel severe plastic deformation at varying temperatures is used to create AZ31 Mg alloy. Several characterisation techniques are used to probe the material's microstructure, texture, and hardness. The effective-strain increases with decreasing temperature, as predicted, mirroring the impact of grain refining. Meanwhile, at higher temperatures, pyramidal  $c + a > slip$  activates more often, and more 1011 contraction twins are born specifically to induce pyramidal  $c + a > slip$ , thereby weakening the base texture. The majority of the grains are sub-structured, and dynamic recrystallization (DRX) may not have been very successful. Hardness readings at 400°C are too low but more stable, whereas the hardness may reach 79.9 HV at 200°C, however, the hardness distribution is the poorest because an interior fracture could emerge, compromising hardness uniformity.

### 3. METHODOLOGY

The method used in this study investigated the effect of different degrees of cold working (rolling) on the bio-corrosion wear properties of magnesium alloy (AZ91) The samples were first heated to 400°C for one hour and then cooled at in the oven The second step consisted of rolling the samples with different thickness reductions of 5%, 10%, and 15%. Microstructure analysis was carried out using optical microscope and SEM to evaluate the effect of cold work on the samples. Wear tests were carried out by simulated body fluid (SBF) absorption of the samples, while bio-corrosion tests were carried out by Tafel test and hydrogen evaluation to measure the corrosion rate by immersing the samples in SBF Different percentages of cold work were selected to examine their relationship with the studied factors. The results showed that increased cold work increased the resistance to damage, modified the microstructure and increased the toughness. In particular, the alloy with 5% cold-rolling percentage had the highest expression than the base alloy and the other rolling percentages, indicating the presence of a range of cold-rolling percentages can be used to obtain a high reference of surgical implants corrosion value and wear resistance. Overall, the methodology used in this study provides valuable insights into the effects of cold treatment on magnesium compounds, which could lead to the identification of biodegradable magnesium implants that provide efficient and biocompatible. The chosen materials for studied in the current work is biodegradable Magnesium alloys (AZ91). The alloy used in the third-generation biomaterials [10]. The AZ91 alloy is cast magnesium alloys typically contents aluminum (9%Al) and a zinc (1%Zn) by weight. Among, AZ91 alloy is the most popular option because to its high strength and great cast-ability. For die-casting, AZ91 alloy has to have better mechanical properties. AZ91 is employed for a variety of commercial applications due to its high strength/weight ratio and outstanding welding qualities in fields as diverse as automotive, electrical, medical, sports, and aerospace [11].

Chemical composition of tested materials (AZ91 magnesium alloys) the chemical composition analysis was done using the x-rays fluorescence's (XRF) in the Ministry of Sciences and Technology (Iraq). The chemicals compositions of magnesium alloys obtained by x-rays fluorescence's (XRF) where the alloy content (9.3%Al, 1%Zn, 0.1%Mn, 0.01%Si, and 0.02%Cu). Archimedes' method was used to determine densities, for AZ91 the average density of three samples found to be 1.7925 g/cm<sup>3</sup>. Since the process of preparing the alloys is done through a commercial company, and to obtain an alloy free from any structural deformations or internal stresses that may affect the course of scientific research, the recrystallization process is resorted to remove any influences that the alloy might have been exposed to during manufacturing or cutting operations. The AZ91 alloy, sample recrystallization process accomplished by heating the samples in furnace at 400°C for 3 hours and then cooled at the furnace [12]. A sample of (AZ91) magnesium alloys has deformed by rolling in room temperature reduce thickness of the sample by passing in the one direction of the rolling machine to deferent ratio (5%, 10%, and 15%) [13].

#### 4. RESULTS AND DISCUSSION

##### 4.1 Microstructure (Optical and electron microscope (SEM))

Initial microstructures that consist of equiaxed-grain with an average grain ~30µm. Which can be an indication of recrystallize state of as-received materials. The AZ91 alloys consists of α-Mg and eutectics phases (Mg<sub>2</sub>Al<sub>3</sub>, Al<sub>8</sub>Mn<sub>5</sub>, and Al<sub>4</sub>Mn) distribute heterogeneous in the Mg matrix [14]. The morphology of eutectics precipitate varies from fines particle to block structure (~6µm). The analyses show aluminum and manganese as their main element, as secondary phase contain mainly Al and Mn, promote the formations of segregation and brittle precipitate as shown in Figure 1. During rolling, microstructural significant changes generated on the initial microstructures of AZ91 alloy, which affected by the deformation's degrees. Figure 2 shows optical microscopes images for AZ91 alloy, with different percentage cold work value from the figures remark the effect of rolling on microstructure orientation. The main microstructure generates for different deformation [15]. Rolling at temperature 25°C generates microstructure with some region of small grain relatively un-deformed (~7µm) surrounded by bigger deformed grains in Figure 3. Where in mechanicals twin preferentially formed and intensified when the deformations degrees increase pointing that the max reduction thickness (between 15%-20%). Since it generates higher grains subdivisions on different region of deform sample, probably involve geometry necessary boundary and slip-induced grains boundary sliding during the grains subdivision mechanism. Which commonly originate in inhomogeneous plastics deformation of polycrystalline material with higher anisotropy's level such as Mg alloy as shown in Figures 4 and 5. However, on cold work deformed with reduction higher than 10%, a massive twins boundary interaction generates double-twin formations and increases the localized stresses concentrations, which is often associated with suddenly failure. Heterogeneous microstructures formed at low strain rates, with areas of tiny untwined grain surround by regions of coarse twinned grain and shear-band, whereas high strain rate promoted the production of twinning and shear bands [16].

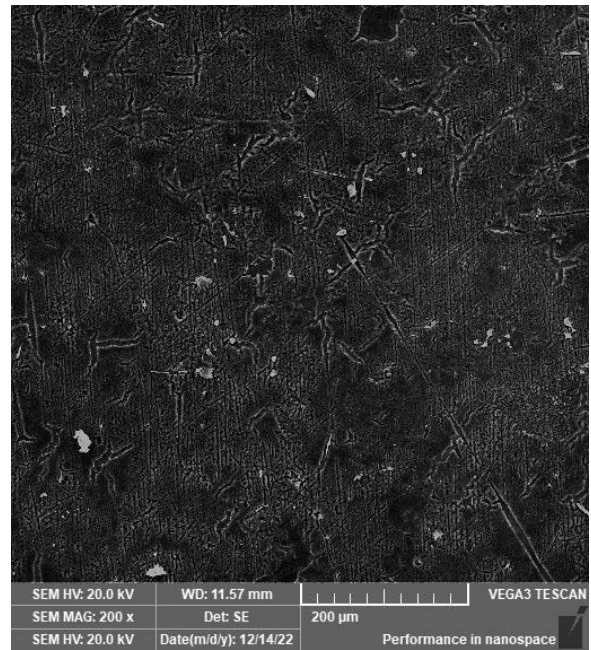


Figure 2. Scanning electron microscope image for AZ91

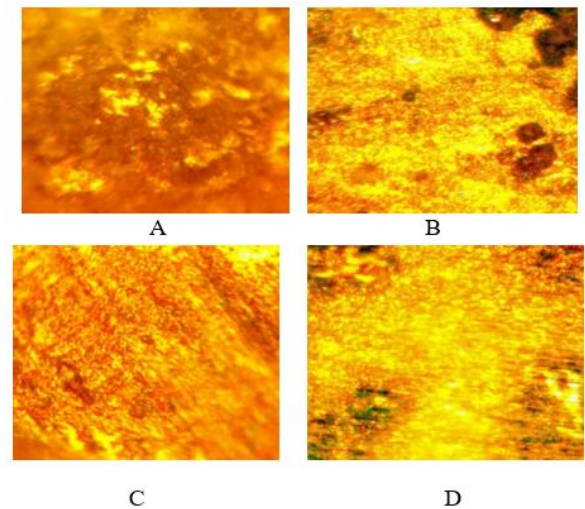


Figure 3. Optical microscope image for AZ91 alloy: A. As received alloy; B. 5% colds work; C. 10% colds work; D. 15% cold work

In this study, the specific and duration temperature of 400°C for one hour was chosen in order to ensure that the samples were annealed and had a uniform microstructure before the rolling process. Annealing is a heat treatment process the heat treatment is heated to a specified temperature and held for a specified time it is necessary to heat the samples to ensure that they are in suitable condition for freezing if the next rolls are used. The rate of cooling of the furnace was not determined in the study. However, it is common practice to allow natural cooling after heating, which involves turning off the furnace and slowly cooling the samples to room temperature because rapid cooling provides heat is generated and characterizes unwanted particles that can affect products. In summary, this study chose a specific temperature and duration of 400°C for one hour to ensure that the samples were annealed and a uniform microstructure before melting the cooling speed in the furnace was not specified, but for natural cooling after cooling to prevent thermal melting and formation of unwanted microstructures, it is common practice.

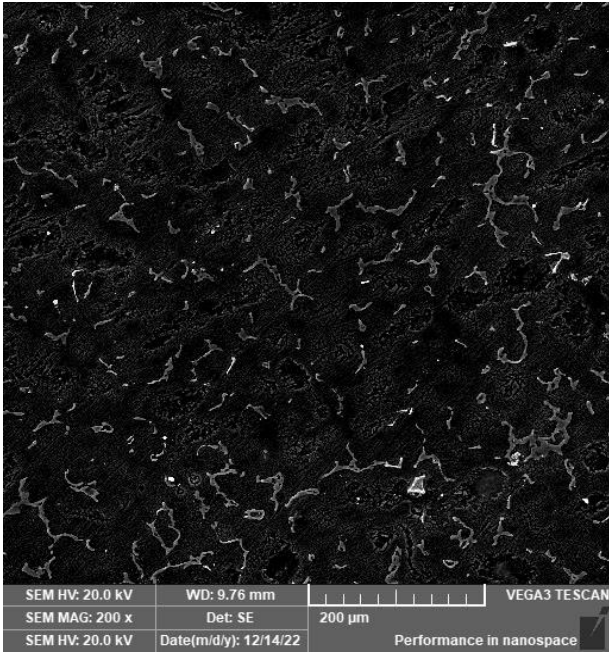


Figure 4. Scanning electrons microscopes images for AZ91 15%

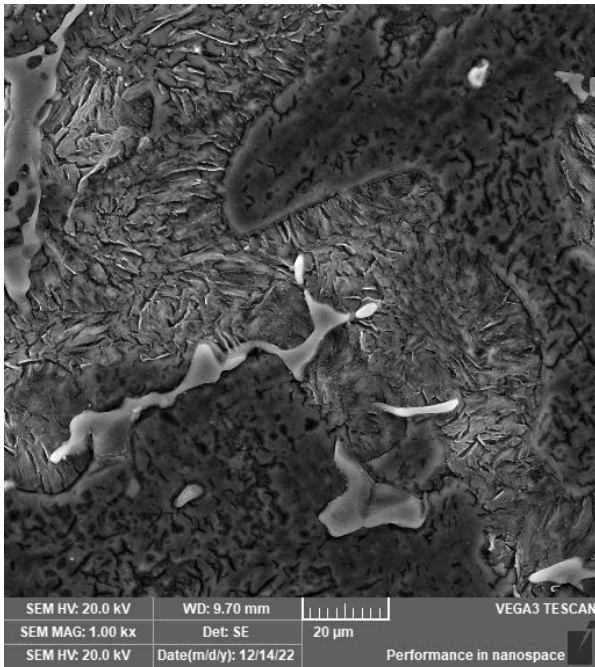


Figure 5. Scanning electrons microscopes image for AZ91 15%

#### 4.2 Hardness test

The impact of cold work on the hardness of AZ91 magnesium alloys is examined. The material's hardness is measured using a Vickers hardness tester set to a holding duration of 10 seconds and weights totaling 200 g. Three separate readings of hardness are collected from various locations on the surface of each sample, and an average is then calculated. As shown in Table 1, the hardness of alloy increased with increase of cold work to maximum value at 10% cold work. The hardness of colds rolling sample increase from (102.79 HV to 122.95 HV) for AZ91. This strengthen mainly influence by the rolling reductions and generate by the activations of various deformations mechanism, include

mechanicals twins, slip on non-basal and basal plane and highs dislocation pile-up produce at grains and small particles boundary of cold rolling. After this percentage, the alloy will have reached the highest stress energy that can be by the deformation mechanisms such as twinning and sliding levels. Therefore, the alloy will have a lower hardness when increasing the forming percentage above 10%, but it will remain higher than the hardness recorded for the basic alloy before forming [17].

Table 1. the hardness test of AZ91 alloy

HV kg/mm <sup>2</sup>	Sample
102.79	AZ91
122.71	AZ91 5%
122.95	AZ91 10%
117.66	AZ91 15%

Table 2. The results for AZ91 alloy samples

	E Corrosion (mV)	I Corrosion mA/cm <sup>2</sup>	BC mv/Decade	Ba mv/Decade
AZ91	-1801	20.91	-36.5	41.4
AZ91 5%	-1606	23.44	-36.1	39.8
AZ91 10%	-1763	27.77	-35.3	44.6
AZ91 15%	-1807	47.2	-36.1	41.2

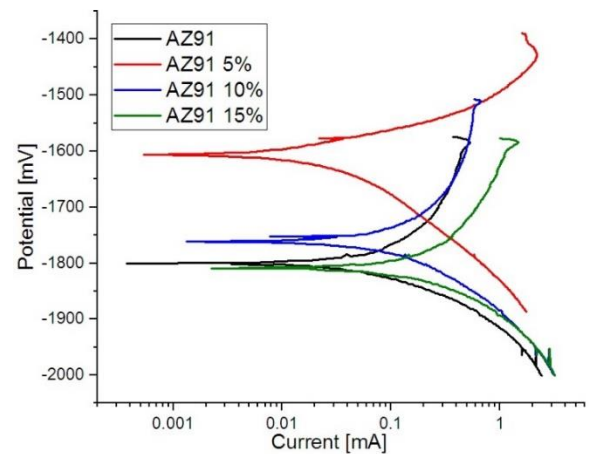


Figure 6. Four samples of AZ91 alloy Tafel test results

#### 4.3 Corrosion

##### 4.3.1 Potential dynamic polarization

The corrosion rate of the samples is determined by immersing them in SBF at room temperature and using the Tafel test. Such experiments may provide an approximation of the electrochemical behavior of the Mg alloys (AZ91) investigated in a corrosive environment. The percentage cold work's impact on the corrosion parameters of corrossions currents density ( $I_{corr}$ ), corrossions potentials ( $E_{corr}$ ), and corrosion rates (CR). As can be seen in Tafel test For AZ91 alloy, we see from Table 2 and Figure 6 that as the formation percentage increases, the potential value decreases, with the lowest value occurring at 5% cold work and gradually increasing to the reserved alloy value at 15% formation percentage. In Alloy AZ91, the second phase ( $Mg_{17}Al_{12}$ ) is an important factor in the corrosion process, as the base alloy in which the second phase is randomly distributed and with

rolling organized on the grains boundary, forming a barrier to corrosion to a certain extent, as this effect appears at a ratio of 5% [18].

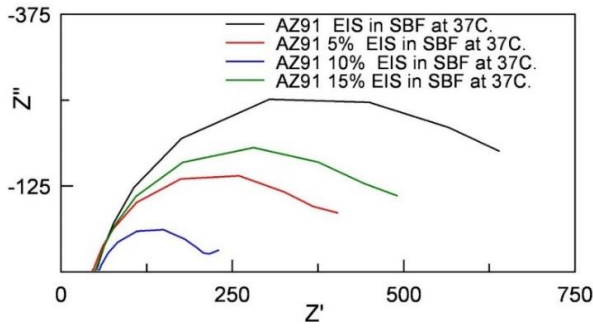


Figure 7. Nyquist test result for AZ91 alloy

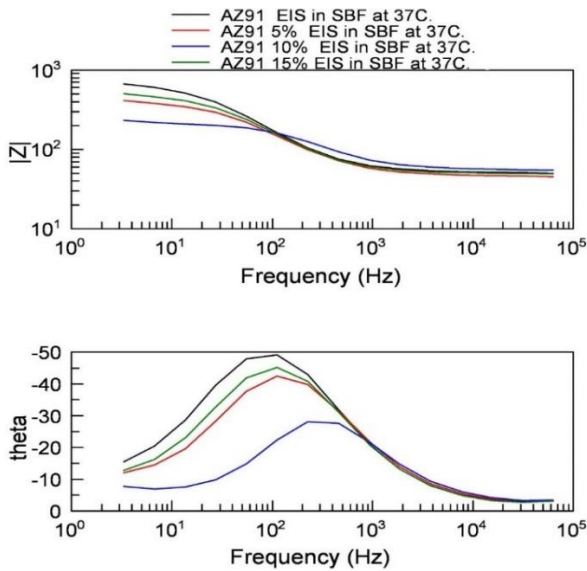


Figure 8. Bode test result for AZ91 alloy

#### 4.3.2 Electrochemical impedance spectroscopy test

Electrochemically characterizations of the surfaces are carried out by using standards three-electrode traditional corrosion cells with SCE as a reference electrode (its potentials vs. SHE is 0.2421 V), two graphitic rods as the counter’s electrodes, and the materials test as working electrodes. The volumes of the cells are 500 ml. The polished samples immerse in preheat simulated body fluid at 37°C for 1800 s to record OCP. EIS was undertaken using a Corr Test Workstation (Corr Test, China). The frequency ranges are 0100 kHz to 015 MHz in perturbations amplitudes 10 mV at 10 points per frequency decades. All EIS tests taken for the surfaces OCP for two times to ensure high reproducibility. Bode plots showed the logarithms of the impedances modulus  $|Z|$  and phase’s angles ( $\theta$ ) as functions of the logarithms of the apply frequency ranges and the EIS data are typical present as a Nyquist plots, where the imaginary’s impedances component ( $Z''$ ) is plotted against the real impedances components ( $Z'$ ) at each excitations frequency [19].

##### (1) Nyquist test

It is the relationship between the resistance and resistance of solution. As shown in Figure 7, the AZ91 has the highest corrosion rates because of high resistance of the obstruction of ion transfer. While the AZ91 10% have the lower corrosion rate.

##### (2) Bode test

It is the relationship between the resistance and frequency. As shown in Figure 8.

#### 4.4 The simple immersion

According to ISO 16428 standard the weight loss value of alloys sample in different cold work percentage immersion in (SBF) at 37°C recording in the Table 3. The value of corrosion rate for alloys various with cold work percentage for both alloys samples as in Tables 3 and 4. This diversity came from the method of interaction of magnesium alloys with the corrosion environment, where magnesium alloys are affected by the variables of temperature, the pH number of the solution and the type of ions, as well as the distribution of the second phase in the alloy and the flow of the fluid as see in Figure 9 AZ91 alloy sample after different immersion time.

These variables directly affect the rate of corrosion and the formation of insulating layers on the surface of the alloy. The study added the variable of internal stresses and deformation with the microstructure of the alloy [20].

Table 3. Weight change to immersion AZ91 alloy samples

Weight Change in Grams	Simple
0.0080	AZ91
0.0063	AZ91 5%
0.0051	AZ91 10%
0.0061	AZ91 15%

Table 4. The mass loss rate of AZ91 sample

MR (g/m <sup>2</sup> day)	Simple
2.2858	AZ91
1.8	AZ91 5%
1.457	AZ91 10%
1.7429	AZ91 15%



Figure 9. AZ91 alloy sample after different immersion time

By use the equation [21]:

$$MR = \Delta m / A \cdot t \quad (1)$$

where,  $MR$ : The mass loss rate;  $\Delta m$ : The mass losses (g);  $A$ : the exposed area (m<sup>2</sup>);  $t$ : the exposure time (days).

Calculated the mass loss rate as in the Table 4.

#### 4.5 Ion released

AZ91 samples are stored in plastics containers with tight lids and expose to the physiological mediums (SBF) for seven days. The solutions held at 37°C with the use of a thermostatic bath. After that, examination the solution and record the result in Table 5. AZ91 alloy, with an increase in the percentage of formation, the amount of liberated ions increases, but in the 10% cold forming, there is drop in liberated ions. As mentioned, the result of ion released are same with immersion test results according ISO 16428 standard [22].

**Table 5.** AZ91 ion released

Mg: Flam eCont Actual	Simple
125.736 ppm	AZ91
141.952 ppm	AZ91 5%
111.700 ppm	AZ91 10%
140.231 ppm	AZ91 15%

#### 4.6 Biological tests antimicrobial activity

Antimicrobial activity investigated using included gram-negative bacteria (*Enterococcus*) and gram-positive bacteria (*Staphylococcus epidermidis*). In diagnostic labs, spreading microorganisms on a surface of alloys samples perform the test. After that incubated at 37°C for 24 hrs. The inhibition areas then evaluated. The test done in the University of Babylon - Faculty of Science for Girls.

After culturing the samples for bacteria and incubating them for 24 hours in the College of Science laboratories, it is found that all samples exhibited the same behavior in the growth of bacteria, indicating that the rolling process had no effect on the results.

#### 4.7 Wear testes results

To study the Tribology behavior of samples, wet sliding wear test carried out following ASTMs G99-050 using a wear tester pin-on-disk. A sample of alloys subjected to wear testing, which done at a constant speed (350rpm), load (5N), and duration (30 min). The wear test conducted in SBF at room temperature. AZ91 alloys sample from Figures 10-13. The sample weight record before and after test and the weight change calculated in Table 6. In general, increasing the cold formation led to an increase in the wear resistance of the used alloys. AZ91 alloy, by increasing the forming percentage, increased the wear resistance to 5%, and it has the highest wear resistance. Then the resistance decreased, reaching 15%. This can be attribute to the stress hardening of the surface of the sample, as it reached the highest resistance at this ratio, but it remained higher than the base alloy.

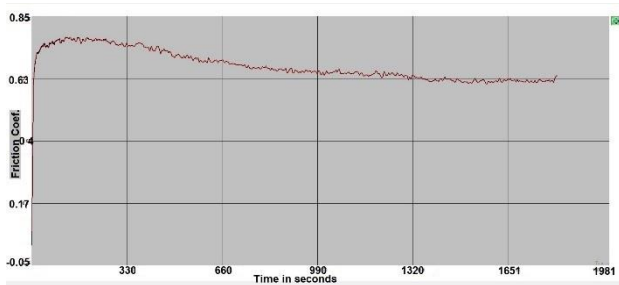


**Figure 10.** The evolution of the coefficient of friction of AZ91

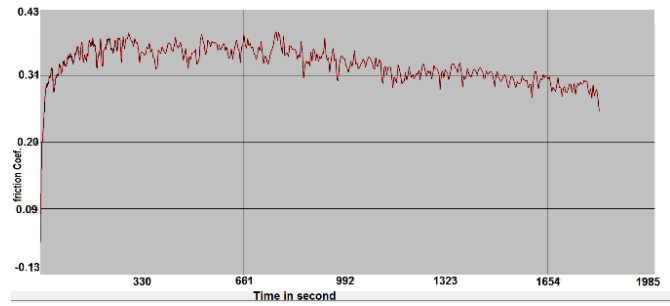


**Figure 11.** The evolution of the coefficient of friction of AZ91 5%

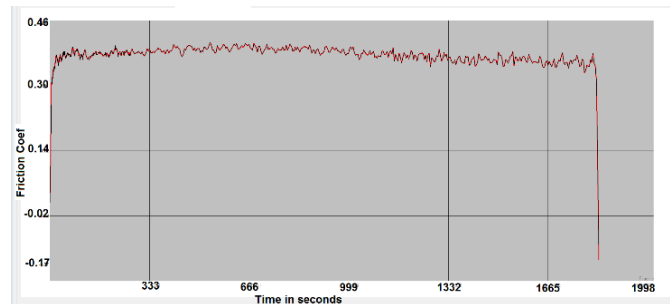


**Figure 12.** The evolution of the coefficient of friction of AZ91 10%

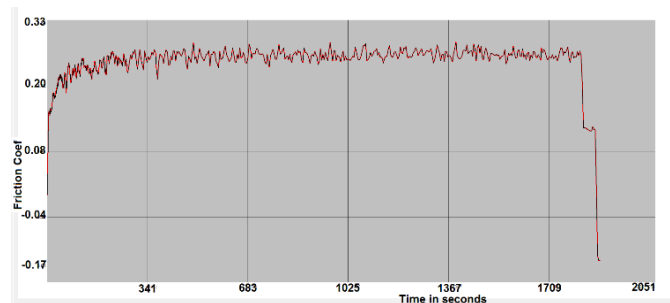


**Figure 13.** The evolution of the coefficient of friction of AZ91 15%

**Table 6.** Weight change for wear test

Weight Change in Grams	Simple
0.0044	AZ91
0.0024	AZ91 5%
0.0036	AZ91 10%
0.0037	AZ91 15%

### 5. CONCLUSIONS

The addition of magnesium compounds as potential biomaterials for biodegradable implants has gained much interest in recent years due to their high specific strength, lightweight nature, cortical bone-like elastic parameters, and high biocompatibility Na aimed to investigate the effect of different cold rates of work (rolling) on biocorrosion wear properties of magnesium alloy (AZ91), showing improved biodegradable magnesium implants with improved performance and biocompatibility The study mainly 5 times rolling process of samples Different thickness reductions of 5%, 10% and % were used to quantify the cold work and then microstructure analysis was carried out by optical microscope

and SEM to evaluate the effect of cold work on the samples. Wear tests were carried out by slitting the samples in simulated body fluid (SBF), while the samples were immersed in SBF and bio-corrosion was tested by measuring the corrosion rate using Tafel test and hydrogen evaluation. These data provide valuable insight into the relationship between cold working rates and resulting changes in magnesium compounds, which may lead to the identification of biodegradable magnesium implants that improve performance and with the natural world meets.

## REFERENCES

- [1] Kainer, K.U. (Ed.). (2003). *Magnesium Alloys and Technology*. John Wiley & Sons.
- [2] Wang, H., Estrin, Y., Fu, H.M., Song, G.L., Zúberová, Z. (2007). The effect of pre-processing and grain structure on the bio-corrosion and fatigue resistance of magnesium alloy AZ31. *Advanced Engineering Materials*, 9(11): 967-972. <https://doi.org/10.1002/adem.200700200>
- [3] Sietsema, W.K. (1995). Animal models of cortical porosity. *Bone*, 17(4): S297-S305. [https://doi.org/10.1016/8756-3282\(95\)00307-Y](https://doi.org/10.1016/8756-3282(95)00307-Y)
- [4] Johnston, S., Shi, Z., Atrens, A. (2015). The influence of pH on the corrosion rate of high-purity Mg, AZ91 and ZE41 in bicarbonate buffered Hanks' solution. *Corrosion Science*, 101: 182-192. <https://doi.org/10.1016/j.corsci.2015.09.018>
- [5] Alsagabi, S., Ninlachart, J., Raja, K.S., Charit, I. (2016). Passivity and localized corrosion of AZ31 magnesium alloy in high pH electrolytes. *Journal of Materials Engineering and Performance*, 25: 2364-2374. <https://doi.org/10.1007/s11665-016-2101-9>
- [6] Abbasi, S., Aliofkhaezrai, M., Mojiri, H., Amini, M., Ahmadzadeh, M., Shourgeshty, M. (2017). Corrosion behavior of pure Mg and AZ31 magnesium alloy. *Protection of Metals and Physical Chemistry of Surfaces*, 53: 573-578. <https://doi.org/10.1134/S2070205117030029>
- [7] Liu, C., Zheng, H., Gu, X., Jiang, B., Liang, J. (2019). Effect of severe shot peening on corrosion behavior of AZ31 and AZ91 magnesium alloys. *Journal of Alloys and Compounds*, 770: 500-506. <https://doi.org/10.1016/j.jallcom.2018.08.141>
- [8] Vaira Vignesh, R., Padmanaban, R., Govindaraju, M. (2020). Study on the corrosion and wear characteristics of magnesium alloy AZ91D in simulated body fluids. *Bulletin of Materials Science*, 43: 1-12. <https://doi.org/10.1007/s12034-019-1973-3>
- [9] Li, M., Lu, L., Fan, Y., Ma, M., Zhou, T., Qi, F., Zhang, H., Wu, Z. (2023). Research on microstructure evolution and deformation behaviors of AZ31 Mg alloy sheets processed by a new severe plastic deformation with different temperatures. *Materials Today Communications*, 34: 105467. <https://doi.org/10.1016/j.mtcomm.2023.105467>
- [10] Zheng, Y.F., Gu, X.N., Witte, F. (2014). Biodegradable metals. *Materials Science and Engineering: R: Reports*, 77: 1-34. <https://doi.org/10.1016/j.mser.2014.01.001>
- [11] Yeh, M.T., Chang, C.T., Wang, J.Y., Lin, H.C. (2012). *Mechanical Properties & Material Processing of Magnesium Aluminum Alloys*. Aml Materials Technology Co. Ltd., Taiwan.
- [12] Won, J.H., Lee, H.W., Min, S.H., Ha, T.K. (2016). Effect of aging treatment on mechanical properties of non-flammable AZ91D Mg alloy. *International Journal of Materials and Metallurgical Engineering*, 9(8): 1071-1074.
- [13] Sakai, T., Utsunomiya, H., Koh, H., Minamiguchi, S. (2007). Texture of AZ31 magnesium alloy sheet heavily rolled by high speed warm rolling. In *Materials Science Forum*, 539: 3359-3364. <https://doi.org/10.4028/www.scientific.net/MSF.539-543.3359>
- [14] Watari, H., Davey, K., Rasgado, M.T., Haga, T., Izawa, S. (2004). Semi-solid manufacturing process of magnesium alloys by twin-roll casting. *Journal of Materials Processing Technology*, 155-156: 1662-1667. <https://doi.org/10.1016/j.jmatprotec.2004.04.323>
- [15] Haghshenas, M., Bhakhri, V., Oviasuyi, R., Klassen, R.J. (2015). Effect of temperature and strain rate on the mechanisms of indentation deformation of magnesium. *MRS Communications*, 5(3): 513-518. <https://doi.org/10.1557/mrc.2015.57>
- [16] Koike, J., Ohyama, R., Kobayashi, T., Suzuki, M., Maruyama, K.J.M.T. (2003). Grain-boundary sliding in AZ31 magnesium alloys at room temperature to 523 K. *Materials Transactions*, 44(4): 445-451. <https://doi.org/10.2320/matertrans.44.445>
- [17] Yasi, J.A., Hector Jr, L.G., Trinkle, D.R. (2010). First-principles data for solid-solution strengthening of magnesium: From geometry and chemistry to properties. *Acta Materialia*, 58(17): 5704-5713. <https://doi.org/10.1016/j.actamat.2010.06.045>
- [18] Winzer, N., Atrens, A., Song, G., Ghali, E., Dietzel, W., Kainer, K.U., Hort, N., Blawert, C. (2005). A critical review of the stress corrosion cracking (SCC) of magnesium alloys. *Advanced Engineering Materials*, 7(8): 659-693. <https://doi.org/10.1002/adem.200500071>
- [19] Cottis, R., Turgoose, S. (1999). *Electrochemical Impedance and Noise*. NACE International.
- [20] Shaw, B.A. (2003). Corrosion resistance of magnesium alloys. In *ASM Handbook, ASM International Handbook Committee: Metals Park, OH, USA*.
- [21] Mena-Morcillo, E., Veleza, L. (2020). Degradation of AZ31 and AZ91 magnesium alloys in different physiological media: Effect of surface layer stability on electrochemical behaviour. *Journal of Magnesium and Alloys*, 8(3): 667-675. <https://doi.org/10.1016/j.jma.2020.02.014>
- [22] Zheng, Y.F. (2015). *Magnesium Alloys as Degradable Biomaterials*. CRC Press.